Atmospheric Research 138 (2014) 139–151

Contents lists available at ScienceDirect

Atmospheric Research

journal homepage: www.elsevier.com/locate/atmos

Cloud cover and UV index estimates in Chile from satellite-derived and ground-based data

A. Damiani [a,*], R.R. Cordero [a], S. Cabrera [b], M. Laurenza [c], C. Rafanelli [d]

[a] Universidad de Santiago de Chile, Departamento de Fisica, Santiago, Chile
[b] Universidad de Chile, Instituto de Ciencias Biomédicas, Santiago, Chile
[c] Institute for Space Astrophysics and Planetology — INAF, Roma, Italy
[d] International Center for Earth Sciences, c/o CNR — Institute of Acoustics and Sensors "O.M. Corbino", Rome, Italy

ARTICLE INFO

Article history:
Received 26 August 2013
Received in revised form 1 November 2013
Accepted 7 November 2013

Keywords:
Satellite
Radiometer
UV radiation
Clouds

ABSTRACT

Data of Lambertian equivalent reflectivity (LER) in ultraviolet (UV)-A range recorded by Total Ozone Mapping Spectrometer (TOMS) series aboard Nimbus 7 and Earth Probe and by Ozone Monitoring Instrument (OMI) on EOS Aura have been analyzed over eight Chilean locations spanning from about 18° to 62° S (i.e. including Profesor Julio Escudero station, Antarctic peninsula), covering years 1978–2011. Generally the distribution of the reflectivity is similar for both TOMS datasets. A slightly better agreement has been found for the most southern locations while a small discordance appears for northern locations. The latter could be partly due to actual differences in the cloud cover conditions. On the other hand, OMI LER data differ from TOMS ones in almost all locations. Daily cloud modification factor (CMF) values from ground-based global solar irradiance measurements have been compared with OMI LER-based CMF data. The northernmost and southernmost locations characterized by prevalent clear sky and winter snow conditions, respectively, showed the worse agreement with a correlation coefficient $r = 0.63$ and 0.71, while other stations showed a better correlation (i.e. $r = 0.83$ and $r = 85$).

Clear sky ground UV index values for Santiago de Chile have been estimated for years 1979–2011 by means of an empirical reconstruction model based on data recorded by a multichannel radiometer. It allowed computing a ground-based CMF for years 1996–2011 and comparing it with satellite data. Results show that OMI CMF based on gridded cell LER data introduces significant differences with respect to equivalent TOMS CMF. On the contrary, the use of overpass LER data allows to evaluate changes in cloudiness and, by using the model, reconstructing the actual UV index. Nevertheless, LER CMF overestimates actual cloud cover conditions in winter. The trend in reconstructed satellite (ground) based UV index during summer months is $+3.3 \pm 0.9\%$ ($+11.9 \pm 2.5\%$)/decade for years 1979–2011 (1997–2011). Further comparisons concerning the Total Cloud Fraction product of Modern-Era Retrospective analysis for Research and Applications (MERRA) suggest that it could be used a further proxy of cloudiness for UV reconstruction models; nevertheless additional analysis is necessary.

1. Introduction

The ultraviolet (UV) radiation reaching the ground plays a fundamental role for human beings, aquatic and terrestrial ecosystems as well as global biogeochemical cycles (Tevini, 1993; Kondratyev and Varotsos, 1996; Slaper et al., 1996; Hader et al., 2007). The adverse effects of the UV radiation on the human skin and eyes as well as its beneficial effects related to the vitamin D production are well known issues (see for example the INTERSUN Programme of the World Health Organization at http://www.who.int/uv/intersunprogramme/

* Corresponding author.
E-mail address: alessandro.damiani@usach.cl (A. Damiani).

0169-8095/$ – see front matter © 2013 Elsevier B.V. All rights reserved.
http://dx.doi.org/10.1016/j.atmosres.2013.11.006

en/). Therefore, monitoring its levels, trends, variability and spatial distribution is an important task usually carried out by means of ground-based observations (e.g. Hicke et al., 2008; Bernhard, 2011; Cordero et al., 2013a). Unfortunately, high-quality UV observations (e.g., Antón et al., 2011c) are somewhat recent and are not uniformly performed all over the Earth. For example few observational sites in the southern hemisphere can claim for a ten-year long time series.

Satellite observations constitute an additional useful tool to monitor UV trends and variability at regional and global scale (e.g., Herman et al., 1999; Ziemke et al. 2000; Ialongo et al., 2011). Nevertheless, because of their reduced temporal and spatial resolution, satellite-based UV index (UVI) estimates only partially fill this gap. The UVI measures the ability of UV radiation to cause erythema in the human skin. It is computed by weighting the spectral solar UV irradiance received on a horizontal surface with the action spectrum for erythema (McKinlay and Diffey, 1987), then integrating over the range 290–400 nm and multiplying the result by 40 m^2 W^{-1}.

Even if the relationship between the total ozone and surface UV levels is a well-understood matter, other parameters such as clouds (Alados-Arboledas et al., 2003), snow/ice (Cordero et al., 2013b) and aerosols (e.g. Kambezidis et al., 2000; Ogunjobi and Kim, 2004) make less reliable satellite UV estimates (e.g., Tanskanen et al., 2007; Ialongo et al., 2008; Buchard et al., 2008; Weihs et al., 2008; Kazadzis et al., 2009a,b; Antón et al., 2010a; Cabrera et al., 2012; Cordero et al., 2013b). A recent work (Damiani et al., 2013) showed that UVI estimates from Ozone Monitoring Instrument (OMI) aboard Aura are usually about 30% higher than actual ground-based UVI values at Santiago de Chile. Both the intense pollution and the complex topography of the region contribute to create the bias and the root mean square error has been shown to be dependent on the sky conditions. Thus, reconstruction methods based on radiative transfer or empirical models are required to build long UV time-series.

In order to run any UV reconstruction model, the first step is to achieve information on ozone and cloudiness. Total ozone column data are worldwide available as overpass or gridded data from the Total Ozone Mapping Spectrometer (TOMS) series and from OMI since 1978. The accuracy of the total ozone column data retrieved from satellite observations is usually within a few percent of the ground-based reference data (e.g., Balis et al., 2007; Damiani et al., 2012). These data provide the total ozone input for running UV reconstruction models.

Usually the effect of the cloud cover on the solar radiation is expressed by means of a cloud modification factor (CMF, dimensionless), defined as the ratio of the measured irradiance at the surface to the calculated cloud-free irradiance. Since long time series in the UV range are typically not available, this information can be derived from global solar irradiance measurements arising from meteorological stations (e.g., den Outer et al., 2005). When this information is not accessible or cloudiness data are needed over a large region, satellite proxies can also be employed. Indeed, efforts were devoted in the past to compare satellite and reanalysis data with actual ground-based cloud cover information (e.g., Eck et al., 1995; Staiger et al., 2010; den Outer et al., 2012).

Following den Outer et al. (2012) we employed Lambertian equivalent reflectivity (LER) values in the UV-A range measured by TOMS and OMI as a cloudiness proxy. The spaceborne reflectivity data returns the radiation reflected by the atmosphere without the Rayleigh scattering contribution (den Outer et al., 2012). Therefore, LER represents the combined cloud, aerosol and surface scene reflectivity as observed from space (Herman et al., 2012). The surface reflectivity in the UVA, in the absence of snow or ice, is typically well below 10% (although high values of surface albedo have been recorded for desert areas e.g. Kleipool et al., 2008), indicating that significant changes in LER are mostly caused by clouds (e.g., Damiani et al., 2013).

In this paper we first evaluate the consistency of LER data recorded by instruments onboard distinct spacecraft over eight Chilean locations. Then, we compare daily CMF from global solar irradiance ground measurements with an OMI LER-based CMF (hereinafter referred to as OMI CMF) covering the period 2005–2011. Following Krotkov et al. (2001) the satellite LER-based CMF (hereinafter satellite CMF) has been computed as

$$CMF = (1-LER)/(1-R_G) \quad (1)$$

with R_G representing the ground reflectivity (see also Tanskanen et al., 2007). The units of reflectivity are frequently given in percent, ranging from 0, for a completely absorbing dark surface, to 100, for a totally reflecting surface. For convenience, we apply a multiplication of 0.01 to all LER values. Differently from den Outer et al. (2012) who simplified the problem taking the satellite CMF equal to 1 − LER, the CMF computed as in Eq. (1) takes into account also the surface albedo that we consider to be constant during the whole year ($R_G = 0.05$).

Moreover, ground-based UVI data recorded at Santiago de Chile for the period 1996–2011 were used to build an empirical reconstruction model of clear-sky UVI values (Madronich, 2007). It allowed the computation of the ground CMF data to validate the satellite CMF values. Reconstructed UVI values computed multiplying clear sky values by satellite CMFs have been firstly compared with actual ground-based UVI observations, then employed to estimate trends in UVI in the period 1979–2011. Finally, an additional analysis is performed, involving the Total Cloud Fraction (TCF) product of Modern-Era Retrospective analysis for Research and Applications (MERRA).

2. Ground and satellite datasets

Ground-based UV observations have been carried out in Santiago de Chile on the roof of the Faculty of Medicine at the University of Chile by using a four-channel filter UV radiometer (Model PUV-510, Biospherical Instruments Inc.) since 1992. Instrument characteristics, calibration details and results of a recent comparison against a double monochromator-based spectroradiometer (i.e. Bentham DMc150) and satellite data have been reported in Cabrera et al. (2012). In this study, otherwise differently stated, we use a dataset of daily UVI values computed averaging 1 min resolution data recorded 1 h around noon.

Daily totals of global solar irradiance measurements were retrieved from the World Radiation Data Centre (WRDC) web site (http://wrdc.mgo.rssi.ru/). In order to minimize calibration problems, we selected only data for the Chilean cities of Antofagasta (−23.65° S, −70.40° W), Santiago (−33.44° S,

−70.65° N), Puerto Montt (−41.46° S, −72.93 W°) and Punta Arenas (−53.16 S, −70.93 W) for years 2005–2011. The data reliability was checked against the recently published McClear model (Lefèvre et al., 2013) exploiting the last results on aerosol, water vapor and ozone achieved by MACC (Monitoring Atmosphere Composition and Climate) project.

Total ozone column and LER data are available for any location from TOMS series for the period 1978–2005 and from OMI for 2004–2013. In the present study we employed the most recent releases of the total ozone data i.e. the TOMS V8 and the OMI-TOMS V8.5. OMI ozone data processed with OMI-TOMS algorithm ensure a somewhat good agreement with previous TOMS time series. On the other hand, the degradation, which affected Earth Probe (EP) TOMS since 2000, has been corrected by an empirical calibration technique in the TOMS V8 data (e.g. Antón et al., 2010b). Some minor discrepancies between these two datasets are related to

i) the different spatial resolution, having the OMI total ozone content (TOC) data a higher spatial resolution than TOMS data;
ii) the solar zenith angle (SZA) dependence in TOMS data which is not present in OMI data;
iii) the ozone retrieval in presence of clouds; while V8 uses the climatological cloud-top pressure based on thermal infrared satellite data, V8.5 uses in situ optical centroid cloud pressure derived with OMI by the rotational Raman scattering method (e.g. Yang et al., 2008). In this way OMI V8.5 derived column amounts have slightly decreased over clouds.

Nevertheless, the main conclusions of the present study are based exclusively on summer data when, particularly for the investigated locations, the SZA is low and the cloudiness is rarely observed.

Assuring a proper long-term accuracy to LER values arising from different satellites is a difficult task (e.g. Herman et al., 2009; Labow et al., 2011). Problems related to the degradation of the photomultiplier scan mirror have been reported for the EP TOMS in particular after 2000. Recent recalibrations allow a somewhat good agreement with other instruments roughly between 40° N and 40° S decreasing towards higher latitudes (Herman et al., 2009). A comparison between EP TOMS LER and ground-based data showed that satellite data are consistent at least up to 2002 (den Outer et al., 2012). Additional problems are related to the photomultiplier detector hysteresis effects in Nimbus 7 (N7) TOMS (Herman et al., 2012); however this issue does not seem to compromise the possibility of using N7 TOMS LER values as a cloudiness proxy (Den Outer et al., 2012).

3. Methodology

The first part of the present paper is devoted to evaluate the inter-satellite consistency of the LER data recorded by N7 TOMS, EP TOMS and Aura OMI over eight Chilean locations characterized by different surface albedo conditions. Then, we compared the daily CMF values, based on ground global solar irradiance measurements performed in four ground stations, with an OMI CMF based on LER data and computed from Eq. (1).

In the second part of the paper, ground-based UVI data recorded at Santiago de Chile for the period 1996–2011 were employed to build an empirical reconstruction model of clear-sky UVI values. Madronich (2007) and Antón et al. (2011a, b) computed the cloud-free UVI through Eq. (2) which takes into account only the total ozone column and the cosine of the SZA.

$$UVI_{clear} = a(\cos(SZA))^{b}(TOC/270)^{c} \quad (2)$$

For SZA between 10 and 60 and total ozone between 200 and 400 DU their method reproduces quite well the actual cloud-free UVI irradiance. As these conditions fit the yearly variations in Santiago, we computed a reliable cloud-free irradiance. The coefficients a, b and c have been computed through the regression analysis of cloud-free ground-based data from January 2006 to December 2007. In this way, the empirical model implicitly takes into account also the aerosol load. Cloud-free data were selected by visual inspection of the 1-min data of the 340 nm channel of the radiometer. Then, we tested the results with respect to data recorded in 2008.

Subsequently, the ground CMF values were computed for the evaluation of the satellite (EP TOMS + OMI) CMF values for this specific location. Finally, the reconstructed actual UVI values have been obtained by multiplying the modeled clear sky values at ground by the previously validated satellite CMFs. Results have been firstly compared with actual ground-based UVI observations, then employed to estimate trends in UVI for 1979–2011, by including also N7 TOMS data.

An additional analysis dealing with the Total Cloud Fraction (TCF) product of Modern-Era Retrospective analysis for Research and Applications (MERRA) has been performed to investigate its potential use as cloudiness proxy for UV reconstruction models.

4. Data analysis

The large latitudinal extension of Chile and the extraordinary heterogeneity of its territory allow assessing inter-satellite differences as a function of cloudiness and land type. Fig. 1 presents the distributions of gridded LER values recorded by N7 TOMS, EP TOMS, and OMI for 1979–2011 above different Chilean locations, spanning from about 18° to 62° S (see the map on the right side). Chile is characterized by desert and semi-arid climate at north (e.g., Arica and Paranal), Mediterranean climate at the center (e.g., Santiago de Chile and Valparaiso), humid and rainy climate towards the south (Castro and Puerto Montt) and ocean-moderated climate in the southernmost tip of South America (Punta Arenas). Moreover, in order to include a polar climate location, Fig. 1 reports also the LER distribution for Profesor Julio Escudero station (see also Cordero et al., 2013b) sited in King George Island, in the so-called Chilean Antarctica Region (not shown in the map). Note that all locations are roughly located at sea level (the only exception being Paranal, sited at 2635 m a.s.l.).

The color map of Fig. 1 refers to the surface reflectivity retrieved from OMI LER data for January (Kleipool et al., 2008). High reflectivity values (more than 0.1) are found in the Northern desert areas, whereas low values (smaller than 0.05) in the South of the country, where vegetation is much more abundant. Finally, intermediate values characterize the central region of Chile around Santiago. The peaks of the distributions

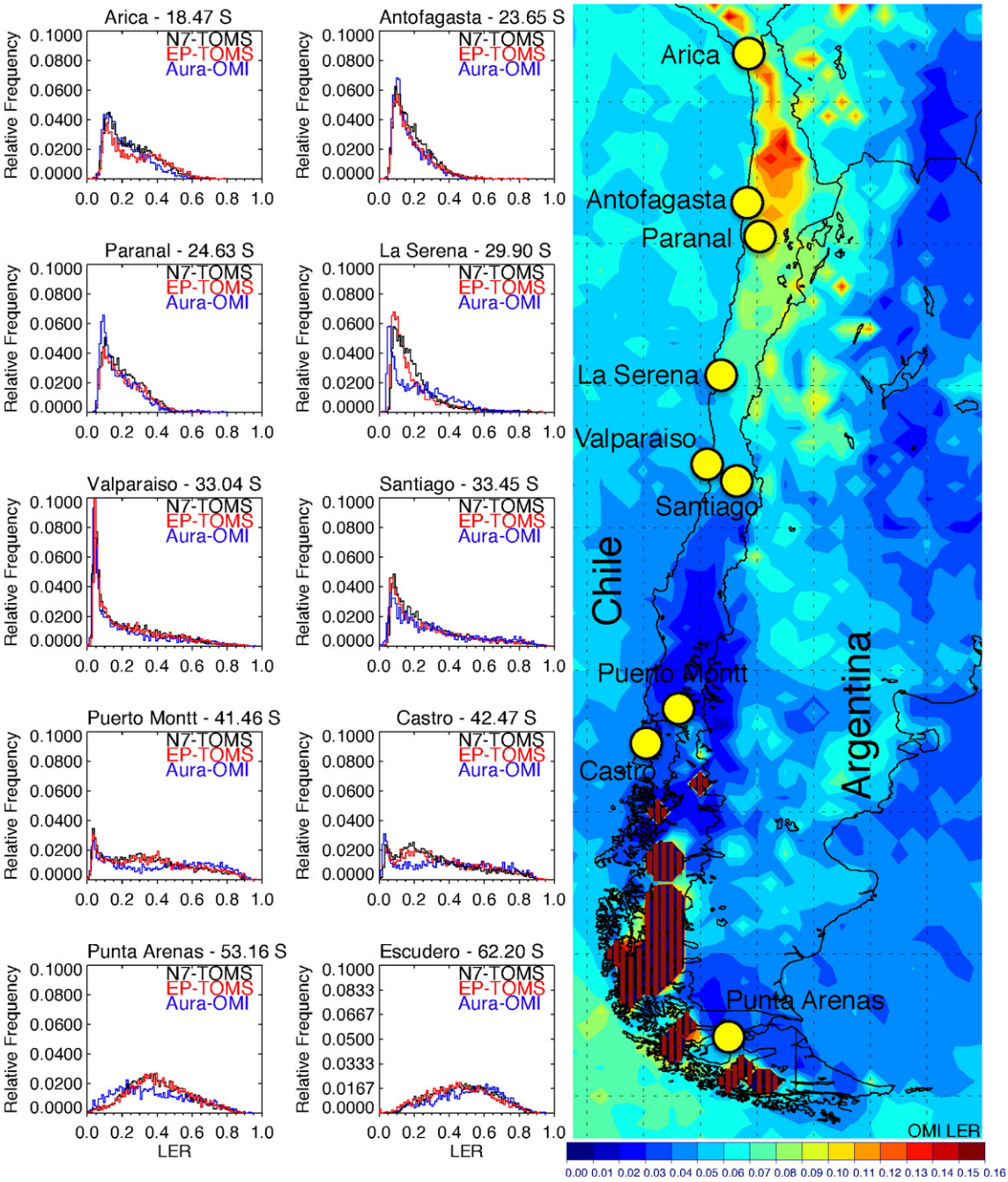

Fig. 1. Distribution of Lambertian equivalent reflectivity (LER) values recorded by TOMS aboard Nimbus 7 (N7) and Earth Probe (EP) for years 1979–1993 and 1997–2004, respectively and by OMI on Aura for years 2005–2011 for eight Chilean locations reported in the map (Escudero base is not shown in the map). The color map depicts the OMI surface reflectivity for January (Kleipool et al., 2008). Dark areas with vertical red lines show values out of the color bar.

(left side in Fig. 1) reflect this behavior and for arid regions they roughly correspond to the surface reflectivity values. It can also be seen that TOMS LER usually peaks roughly in correspondence of OMI LER, with some exceptions (e.g. La Serena).

Fig. 1 shows an overall good match between N7 and EP TOMS datasets, despite they cover different periods (N7 spans from 1979 to 1993 and EP from 1996 to 2005). This confirms that the recently implemented recalibrations in EP LER data (Herman et al., 2009) made them at least consistent with N7 values. Generally, the two TOMS datasets for center-south locations seem to agree somewhat better than for northern regions. For example, both TOMS distributions are almost identical for Punta Arenas and Escudero stations. Taking into account the issues affecting both instruments (i.e. Herman et

al., 2009, 2012), this is an important element to highlight and it suggests that no evident changes in cloudiness occurred in these locations during 1979–2005. On the other hand, the minor differences between N7 and EP TOMS datasets for the northern locations (e.g. Arica, Antofagasta, La Serena) are probably related to actual differences in cloudiness during the two different periods. Indeed, in this region we could expect large inter-annual variations in cloud cover frequency, connected to different phases of the El Nino-Southern Oscillation (ENSO) (e.g. Montecinos and Aceituno, 2003). Therefore, differences in the N7 and EP TOMS distributions could be linked to the different ENSO effects in different periods (see also Herman et al., 2009).

On the other hand, Fig. 1 seems to confirm previous findings for European locations (Den Outer et al., 2012), i.e. OMI LER generally peaks higher than TOMS LER. This behavior is evident for the most northern latitudes (e.g. Antofagasta and Paranal), but not uniformly present at all locations; hence a contribution from actual cloud changes cannot be excluded. Nevertheless, differences between OMI and TOMS involve even the shape of the distribution, in particular for the southernmost locations: LER peak at Punta Arenas (Escudero station) moves from about 0.3 to 0.2 (0.45 to 0.65) for TOMS and OMI, respectively. Such abrupt change in LER can be hardly caused by actual variation in cloudiness.

Both N7 TOMS and OMI LER values have been used in the past to compute the Earth's surface reflectance climatology. Kleipool et al. (2008) showed that the average difference between these LER climatologies is 0.01 for the Northern Hemisphere and 0.02 for the Southern Hemisphere. Moreover OMI surface reflectances are at least 0.04 higher than TOMS over polar cap regions. They speculated that the different periods on which the two climatologies are based (i.e. actual changes in cloudiness) and/or the different overpass times (OMI: 13.45 pm; Earth Probe TOMS: 11.16 a.m.; Nimbus TOMS: 12.00 p.m. equator crossing time) could play some role. Nevertheless, taking into account the very similar LER distribution for both TOMS datasets (i.e. covering different periods and build with data recorded at different overpass times) we discard this hypothesis and focus on other inter-satellite differences.

We remind that the size of the used gridded cell is almost similar for TOMS and OMI (1° × 1.25° for TOMS vs. 1° × 1° for OMI, lat × lon), while the pixel size on which the cell data are based is quite different (at nadir 50 km × 50 km, 39 km × 39 km, and 13 km × 24 km for N7, EP, and OMI, respectively). Damiani et al. (2013) reported some clues of a possible influence of the swath position (i.e. viewing angle) on OMI data, with a somewhat distinct behavior for the most outer swath-angle positions. Moreover, OMI data contain a higher percent of readings recorded under high viewing angles with respect to TOMS; it is reasonable to suppose that these elements can play a role in the discrepancy between OMI and TOMS (see also Den Outer et al., 2012).

In order to investigate the reliability of satellite LER data as a proxy of cloudiness, we compared OMI CMF computed as in Eq. (1) with ground CMF data from global solar irradiance measurements recorded at four Chilean locations (i.e., Antofagasta, Santiago, Puerto Montt and Punta Arenas; see Fig. 1) for 2005–2011. In order to achieve the ground CMF, we computed the cloud-free daily totals of global radiation by means of the recently published McClear model (Lefèvre et al., 2013), exploiting the last results on aerosol, water vapor and ozone achieved by MACC (Monitoring Atmosphere Composition and Climate) project. Therefore, we directly compared this ground CMF with OMI CMF. Although we are aware that further (minor) corrections should be necessary to make an optimal comparison with respect to the satellite CMFs computed for the UVA (i.e. the UV irradiance is expected to be less sensitive to clouds than the global radiation as a result of the substantial amount of scattered UV radiation, see den Outer et al., 2005), we stress that here we focus on the relative differences among different stations and satellite.

As shown in Fig. 2, a good agreement was found for Santiago and Puerto Montt, whereas a minor correlation coefficient (r) is present for both Punta Arenas ($r = 0.71$) and Antofagasta ($r = 0.63$). This could be due to the contribution of many factors so we can only make some speculations. For example, we could expect reduced agreement for Punta Arenas due to snow presence in winter, affecting the reliability of the OMI CMF. Nevertheless, when removing the winter months from the scatter plot, the correlation is even smaller. As discussed in Den Outer et al. (2012), an important element determining the agreement between daily ground CMF and OMI CMF is the wind speed and hence the cloud drifting. The daily cloud drifting, captured by the ground observations, should be mostly contained through the area of the satellite gridded cell. Under wind speed conditions of less than 10 m/s, the usual TOMS gridded cell is the optimal area representative of the daily cloud cover changes (Den Outer et al. 2012). Faster wind speed is expected at Punta Arenas that could contribute to decrease the agreement between satellite and ground data, while lower speed at Antofagasta. In this case, the reasons for the small correlation should be found in its peculiar location, at the boundary between the desert and ocean (i.e., between high and low reflectivity), and in its complex topography.

As we are mainly interested in estimating the surface UV irradiance in the past, we focus on Santiago de Chile, where accurate ground-based surface UV measurements are available.

A previous work (Den Outer et al., 2012) reported that, in order to make satellite (i.e. TOMS and OMI) gridded LER values a good proxy of the cloudiness estimated by ground radiometers, some corrections for OMI data are mandatory. Fig. 3 shows the distribution of LER values from N7 TOMS, EP TOMS and OMI over Santiago for both gridded cell and overpass data. While TOMS datasets remain very similar to each other for both gridded and overpass data, OMI shows a different behavior, the overpass values peaking much higher than gridded data (see also Den Outer et al., 2012). Moreover, an additional feature is the peak shifting in LER values for distinct satellites, i.e. N7 TOMS peaks at around 0.09, EP TOMS at 0.08 and OMI at 0.07. LER data contain information on the surface albedo, clouds and aerosols. In particular, absorbing aerosols contribute to enhance LER reflectivity values. Therefore, this little shift could be a clue of the improved pollution conditions experienced by Santiago during the last decade (see Cabrera et al., 2012 and reference therein).

In order to understand which resolution (i.e. gridded cell or overpass) of satellite data is more representative of the actual cloud cover conditions in Santiago, we need a reference ground-based CMF. Since the satellite overpass time over Santiago is usually close to local noon, we used ground UVI data averaged 1 h around noon along with the clear-sky UVI values, from 1996 to 2012, computed by the empirical model (2), to

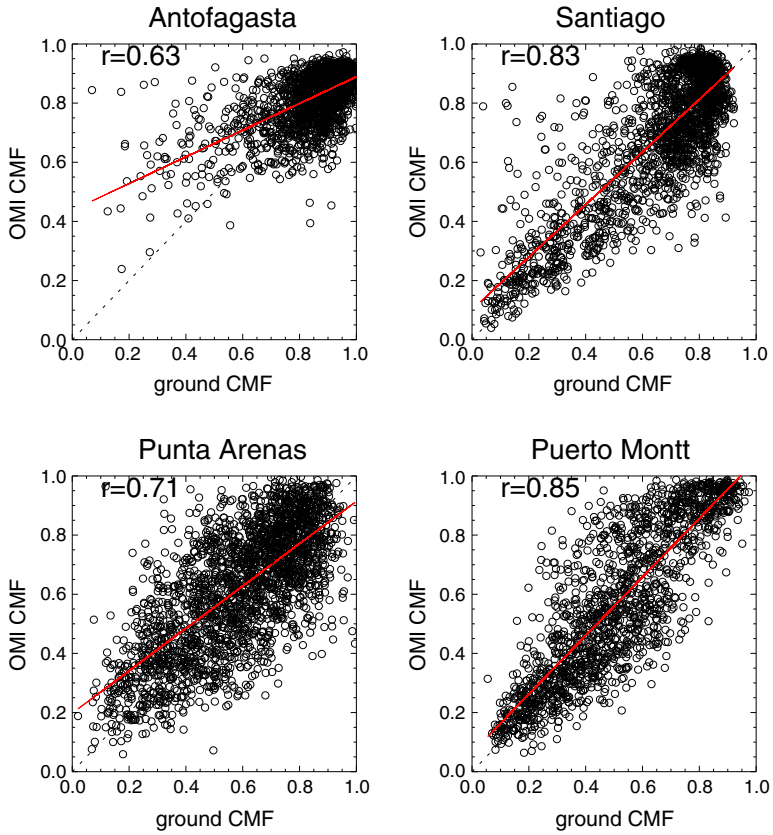

Fig. 2. Scatter plots, regression lines and coefficient of correlations between OMI CMF based on LER values and ground CMF computed from global solar irradiance measurements for four Chilean locations (see the text for details).

calculate an hourly ground CMF. The coefficients in Eq. (2) have been computed through the regression analysis of cloud-free ground-based data for 2006–2007. Then, we tested the results with respect to year 2008.

The bottom panels of Fig. 4 show the scatter plots between clear sky observations and model results for both 2006–2007 and for 2008. The regression coefficient, regression equation, and number of samples are also presented. A good agreement between model and observations for both 2006–2007 and the test period (i.e. 2008) is shown.

The upper panel of Fig. 4 reports the temporal evolution of the ground-based UVI data and the clear sky UVI values computed as in Eq. (2). Usually clouds are present mainly during winter while clear sky conditions and some sporadic clouds characterize summer periods.

In order to compare the ground CMF at noon with the satellite CMF, it is interesting to assess how much the CMF at noon is representative of the total daily ground CMF. The scatter plot between the ground CMF at noon and the ground daily CMF for the period 2006–2007 is depicted in Fig. 5. The

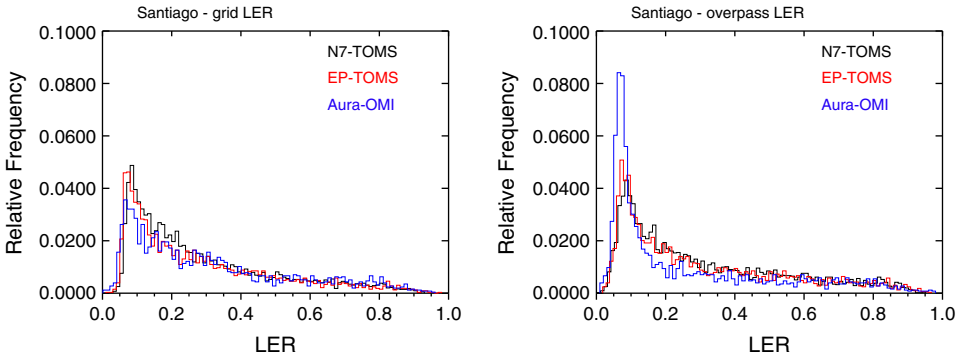

Fig. 3. Distribution of Lambertian equivalent reflectivity (LER) values recorded by TOMS aboard Nimbus 7 (N7) and Earth Probe (EP) for years 1979–1993 and 1997–2004, respectively and by OMI on Aura for years 2005–2011 at Santiago de Chile. Left panel: gridded data; right panel: overpass data.

high correlation (r ~ 0.95) between the two datasets indicates that the CMF at noon is actually representative of the daily cloud cover conditions and suggests that also the satellite CMF should reproduce quite well the daily sky conditions.

Fig. 6 shows the ratio between ground and satellite (EP TOMS + OMI) CMF for 1997–2011 by using overpass (upper panel) and gridded (bottom panel) data. Linear trends and slope values are also reported. When using satellite gridded (overpass) data a somewhat better (worse) day-to-day correlation between ground and TOMS data exists ($r = 0.82$ and $r = 0.76$ for gridded and overpass data, respectively; correlations not shown) while the day-to-day correlation between ground and OMI remains almost the same independently from the spatial resolution of the data ($r = 0.78$ and $r = 0.79$ for gridded and overpass data, respectively; correlations not shown). Nevertheless, Fig. 6 shows that using satellite gridded cell values introduces a positive trend in the ratio pointing to the necessity of including some correction to OMI data (den Outer et al., 2012). In contrast, the upper panel of Fig. 6 suggests that the agreement between OMI and TOMS improves if satellite overpass data are selected. Therefore, we do no attempt to correct OMI gridded data but, despite their smaller correlation, in the following we will focus only on satellite overpass data.

The upper panels of Fig. 7 show the scatter plots between the monthly ground and satellite CMF for 1996–2011 (left) and for EP TOMS (right) and OMI (central) periods, separately. The correlation coefficient (around 0.9) points to a sufficient correspondence between the two datasets, both for the whole period and for separated ones, being slope of the regression lines close to the unity. When we do not include the period 2000–2004 (because of EP TOMS issues, see Herman et al., 2009 and den Outer et al. 2012) correlations remain similar (not shown). The lower panel of Fig. 7 presents the scatter plots between UVI recorded by ground-based observations and the UVI computed by means of the empirical model as in Eq. (2) multiplied by the satellite CMF. In general, we note a fairly good agreement which points to the possibility to reconstruct monthly UVI values exploiting both TOMS and OMI LER datasets.

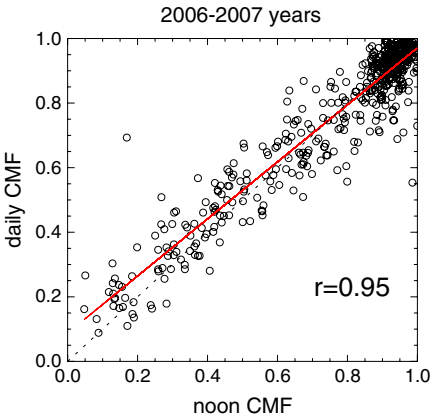

Fig. 5. Scatter plot between ground-based CMF computed for 1 h around solar noon and daily total CMF.

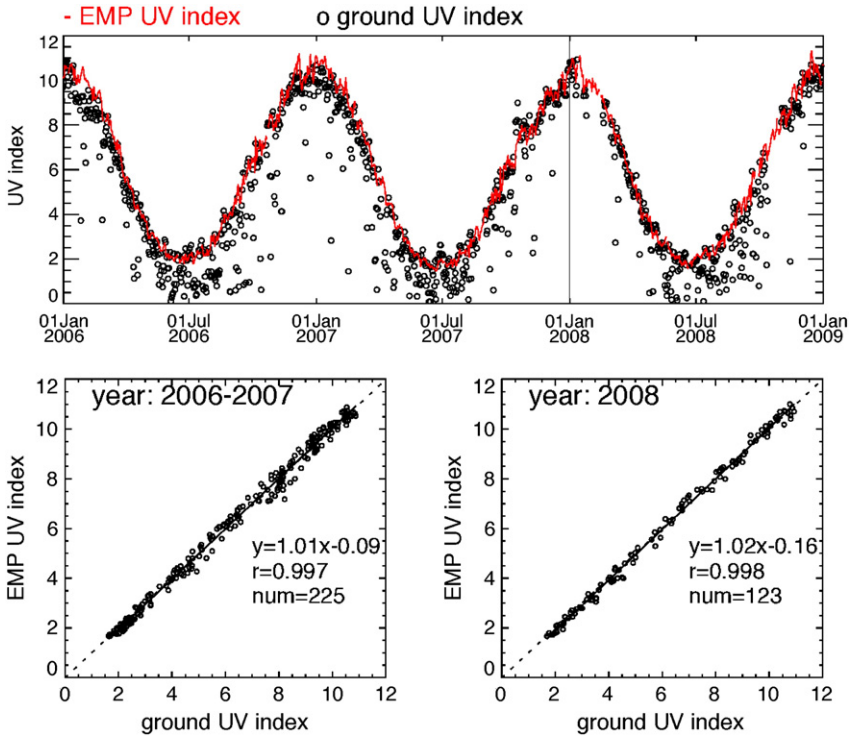

Fig. 4. Upper panel: ground-based UV index values (black circles) recorded by the multichannel UV radiometer at Santiago de Chile and clear-sky UV index values (red circles) computed by an empirical model for years 2006–2008. Lower panels: scatter plot of clear sky UV index from ground data and empirical model for years 2006–2007 (left) and for the test period (right).

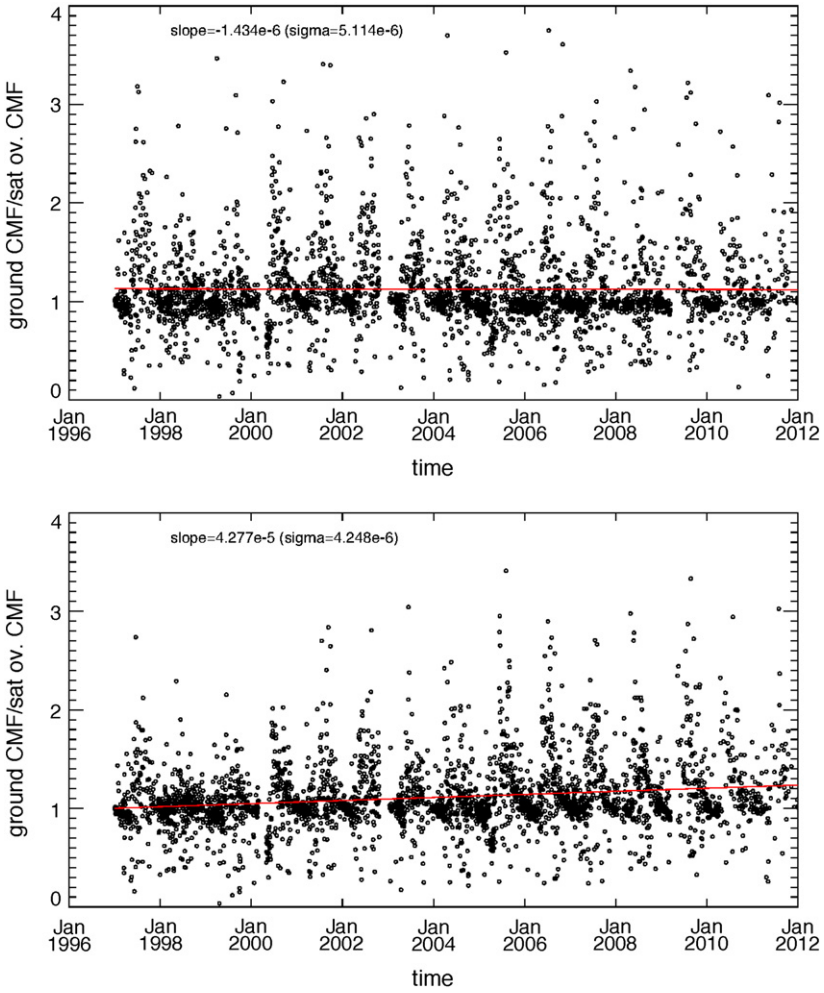

Fig. 6. Ratio between ground and satellite CMF based on overpass (upper panel) and gridded (bottom panel) data over Santiago. EP TOMS data: years 1997–2004; OMI data: years 2005–2011.

Retrospective-analysis (or reanalysis) is a synthesis of the observations and model physics. Although reanalyses have different cloud prediction schemes, usually they do not assimilate cloud fraction directly from observations (Chernokulsky and Mokhov, 2012). Hence, we achieved a further independent information on cloudiness at Santiago by using data from MERRA reanalyses. MERRA is based on the Goddard Earth Observing System (GEOS) data Analysis System version 5 (e.g. Bosilovich et al., 2008) and utilizes a maximum random cloud overlap approach (e.g. Zib et al., 2012). Diversity from Staiger et al. (2010) that used the ratio between shortwave net solar radiation for cloudy conditions and for assumed clear sky conditions from the European Centre for Medium-Range Weather Forecasts (ECMWF) 45 year reanalysis ERA-40 as a cloud proxy, here we employed the Total Cloud Fraction (TCF; TCF = 0 clear sky, TCF = 1 overcast sky) product of MERRA. The CMF from MERRA data computed as in Staiger et al. (2010) present almost the same correlation with the ground observations than using the TCF product, but clouds result optically too thin (i.e. bias with ground observations). It is worthwhile to note that the same behavior has been pointed out for the ECMWF reanalysis (Bromwich et al., 2007; Staiger et al., 2010). Therefore, we decided to transform the TCF to a MERRA-based CMF as follows:

$$\text{MERRA CMF} = (1-\text{TCF})^{0.84} \quad (3)$$

(in the following MERRA UVI indicates the MERRA CMF multiplied by reconstructed clear sky UVI).

Previous papers (e.g., Kylling et al., 1997; Lindfors et al., 2007) pointed out that the transmittance of radiation through a cloud layer is wavelength dependent and differences depend on the SZA. Therefore, to better reproduce the cloud transmittance in the UV range, we introduced a minor correction (i.e. a power index of 0.84) to the original TCF data, as in Matthijsen et al. (2000).

The upper (bottom) panels of Fig. 7 show, in red color, the scatter plots and linear regressions between ground CMF (UVI) and MERRA-based data. The cloudiness information from MERRA is comparable to LER, suggesting to exploit also this product as a cloud proxy for surface UV reconstruction models. Similar results have been obtained with ERA Interim reanalysis

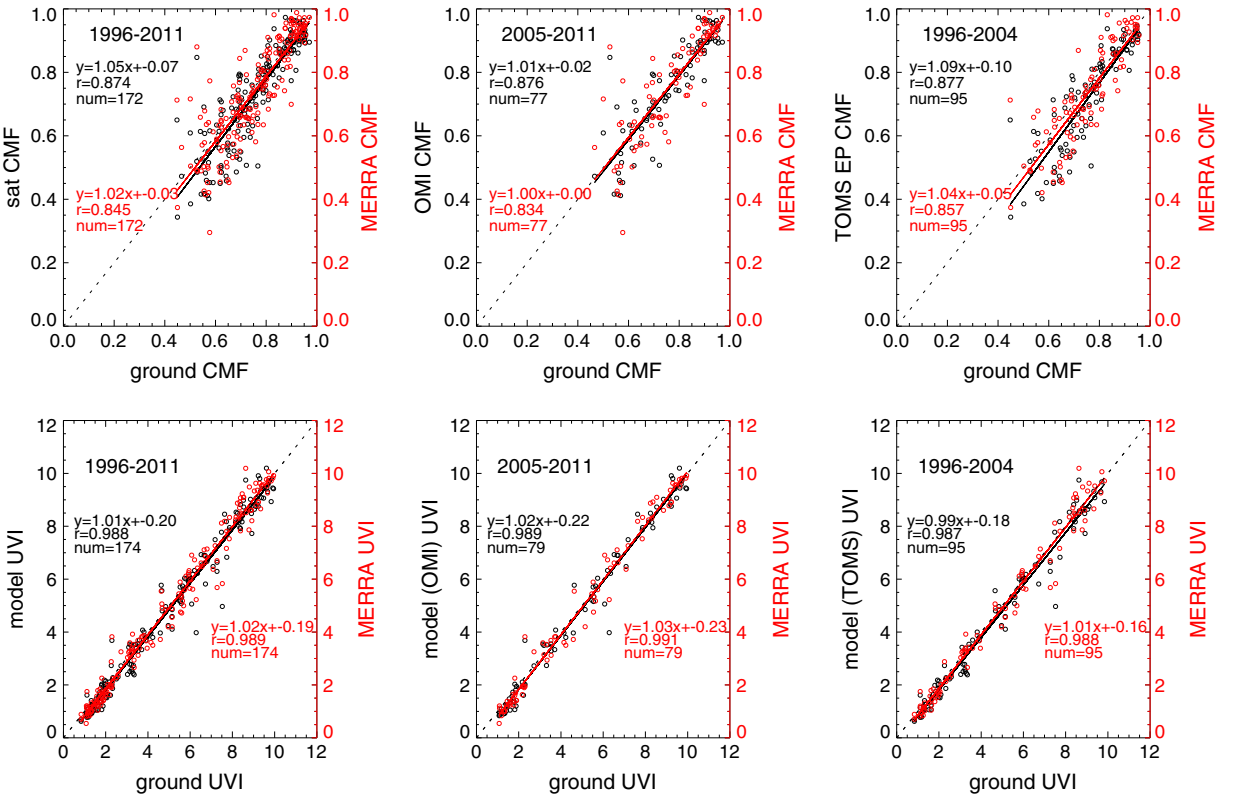

Fig. 7. Upper panels: scatter plots between monthly ground and satellite (MERRA) based CMF for different periods are reported in black (red). Bottom panels: scatter plots between monthly ground and satellite (MERRA) based UV index are reported in black (red). Linear regression lines and equations, coefficients of correlation and number of samples are also shown.

data (not shown). A carefully evaluation of this product based on comparisons with a large number of ground stations is necessary, but it is beyond the scope of this paper.

The upper panel of Fig. 8 shows the total ozone column from TOMS series and OMI at Santiago for the period 1978–2012. In agreement with other published results (see WMO, 2007) we note a noticeable O_3 decrease in particular during 1980–90 years; then the values seem to stabilize.

The middle panel of Fig. 8 shows the monthly CMF based on both ground data and satellite LER values. In addition, we report also the MERRA CMF. Satellite LER CMF matches quite well the ground CMF and reproduces both the yearly and inter-seasonal variability. Nevertheless, the satellite CMF presents an overestimation of the actual cloud cover in winter. The largest winter discrepancies occur during 2000–2004, when the calibration problems occurred. MERRA CMF reproduces quite well both the ground and LER CMF; relative differences with respect to LER CMF (see the blue line) are generally about $\pm$20%. Also in this case, larger discrepancies seem to appear for 2000–2004, mainly in winter.

Finally, the bottom panel of Fig. 8 shows the ground-based UVI data and the UVI values reconstructed with LER and MERRA proxy. Both reconstructed datasets underestimate UVI values in winter.

Fig. 9 shows the monthly averages of the CMF for both ground and satellite and their relative differences (in %) for different periods. Both EP TOMS and OMI CMF present an overestimation of the ground cloud cover of about 0.1 (20%) in winter. During the other months, the agreement with the ground CMF is almost good for OMI while TOMS presents a further smaller overestimation of the ground cloudiness in spring. When the period 2000–2004 is not considered, the general behavior is similar, but differences between ground and TOMS CMF data are smaller in particular for the winter months July, August and September (see the bottom panels).

Leaving aside the necessity to provide some correction to satellite data, especially under high SZA conditions, in order to make them consistent with the ground CMF, part of these differences could arise from the assumption of a constant albedo (0.05) throughout the year in Eq. (1). During winter the possible bright snow over the mountains around Santiago could enhance the total reflectivity of the pixel area causing a seasonal dependence. This is roughly confirmed by the reflectivity climatology used by OMI showing smaller values in summer and higher in winter. This element could be more important for TOMS than OMI, due to the larger pixel size of TOMS. Hence, the TOMS underestimation of the ground CMF in spring could be related to the seasonal dependence in the surface albedo. The fast reduction of the winter snow coverage occurred in this region during the last years could also play a role in reducing this effects in the case of OMI data.

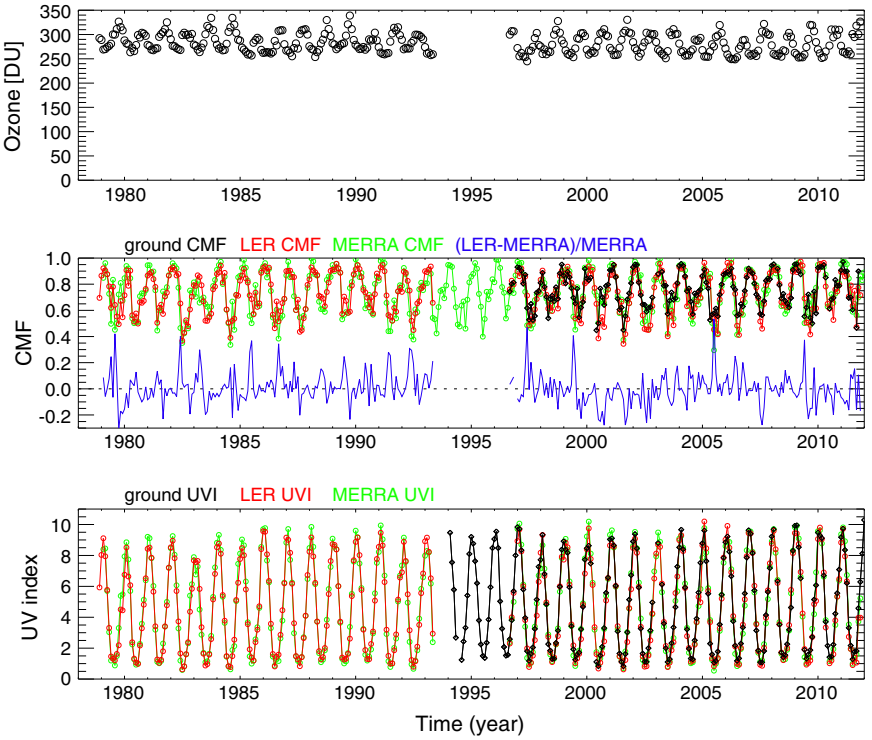

Fig. 8. From up to bottom: time series of monthly total ozone column; time series of monthly ground (black), LER (red) and MERRA (green) based CMF (the relative differences (violet) between LER and MERRA are also shown); time series of monthly ground (black), LER (red) and MERRA (green) based reconstructed UV index for years 1979–2011 (see text for details).

We point out that implementing corrections in the surface albedo values, the satellite CMF data should result empirically corrected. Indeed, by including a seasonal variation in the surface reflectivity, the differences shown in Fig. 9 are almost removed. For example, differences between ground and satellite CMF in winter could be strongly reduced assuming a surface albedo of about 0.15 for winter months, while differences in spring months for TOMS could be removed by means of an albedo value slightly higher (e.g. 0.08) than the employed one (0.05). Even if the correction is not expected to substantially improve the correlation coefficients, it should reduce the bias between the two datasets.

Because of the issues mainly related to the winter data, Fig. 10 shows the time series of the annual summer (January, February and March) averages in CMF and UVI along with their linear trends and slopes for ground-based, satellite and reanalysis data. The sigma values associated to each trend refer to the sampling uncertainty. The linear long-term trends were obtained as least squares fits of the annual summer mean values. Their significance was estimated through Fisher's test at the 95% confidence level. Den Outer et al. (2012) showed the coherence of N7 TOMS LER data with EP TOMS LER at least for Europe. Because of the shortness of our dataset, we cannot check the reliability of N7 TOMS with respect to the ground observations for Santiago; nevertheless we note the very good agreement between LER and MERRA data during the investigated period. Both datasets capture the year-to-year variability of the ground-based measurements.

The slightly positive trends in reconstructed CMFs for 1979–2011 are found to be not statistically significant. Ground data for 1997–2011 show a positive trend of 7.1 $\pm$ 2.4% and 11.9 $\pm$ 2.5% per decade for CMF and UVI respectively, both statistically significant. Smaller CMF values in 1983 and 1998 correspond to strong El Niño events; the latter event likely drove the large positive trends in ground data. Finally, the trends of reconstructed UVI values based on LER and MERRA data for 1979–2011 years are 3.3 $\pm$ 0.9% and 3.2 $\pm$ 0.9% per decade respectively and are both statistically significant. The positive trends in UVI indicate an increase of erythemal doses during summer, which is mainly guided by the lower ozone values during the last two decades with respect to years 1978–1985 (see Fig. 8). The similar trend values in UVI using either LER or MERRA cloudiness proxy stand for the exactness of the above conclusions and suggest the potential use of MERRA TCF in surface UV reconstruction models.

5. Conclusions

Grid cell data of Lambertian equivalent reflectivity (LER) in UVA recorded by N7 TOMS, EP TOMS and OMI Aura during the period 1978–2011 have been analyzed over eight Chilean locations, including Escudero station (Antarctic peninsula). Generally, the distribution of the reflectivity is similar for both TOMS datasets with small discordances appearing for northern locations. This could be due to actual differences in the cloud cover conditions occurring during the different

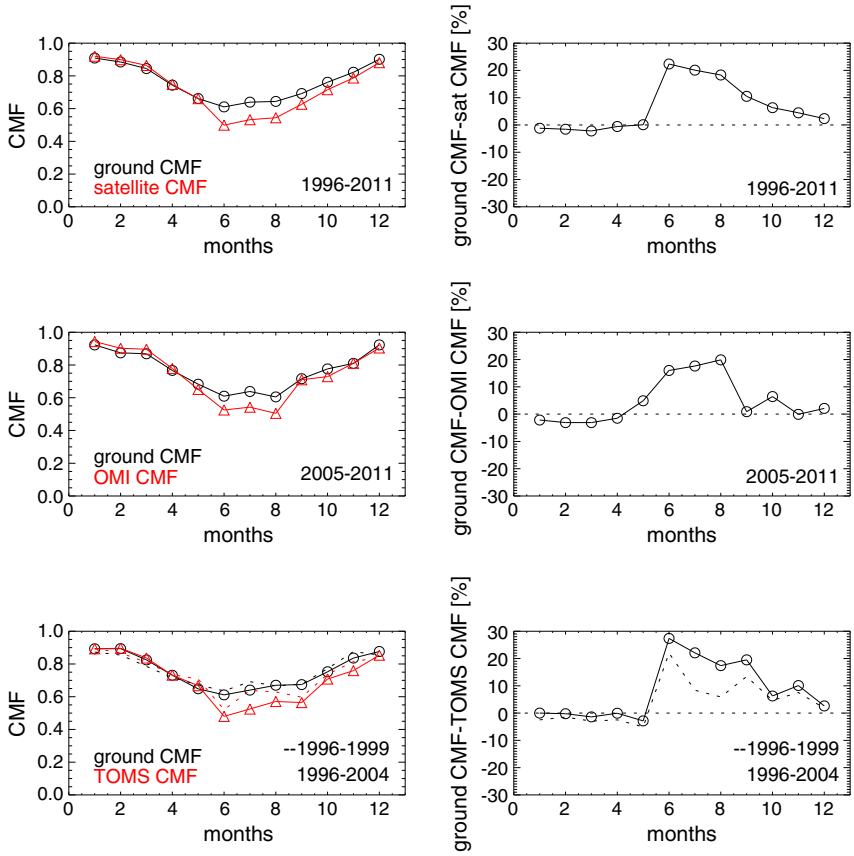

Fig. 9. Left column: monthly mean ground-based CMF (black) and LER-based CMF (red) for OMI and EP TOMS datasets. Right column: relative differences ((ground-satellite)/satellite in %) in CMF for OMI and EP TOMS datasets.

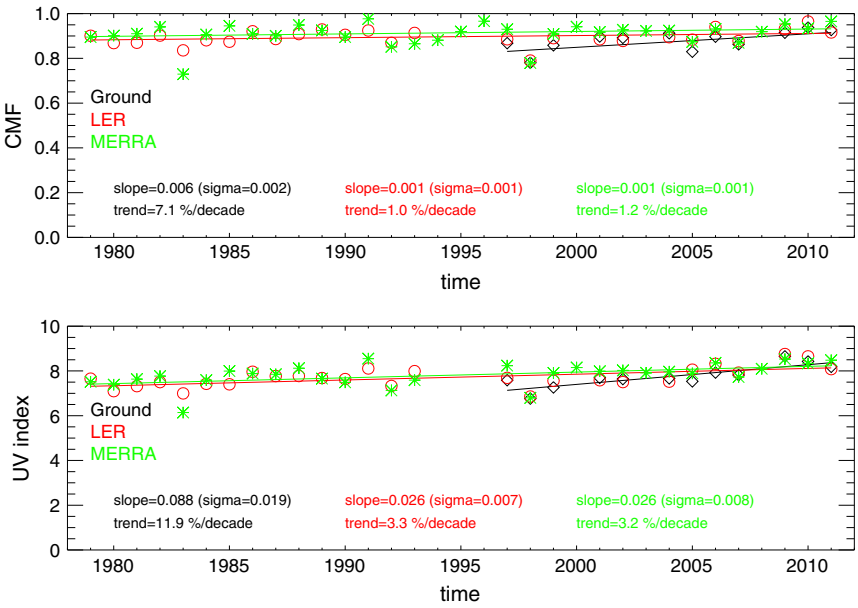

Fig. 10. Time series of annual summer (January, February and March) averages for CMF (upper panel) and UV index (bottom panel) estimated by ground-based observations (black) and satellite LER (red) and MERRA reanalysis (green) data. Linear trends and slopes are also shown.

periods (1978–1993 for N7 and 1996–2005 for EP) and caused, for example, by different ENSO phases. On the other hand, OMI data differ from TOMS data for almost all locations, possibly related to differences in the geometry of the instruments.

Daily cloud modification factor (CMF) from ground-based global solar irradiance measurements was compared with the OMI LER-based CMF for 2005–2011. The northernmost (southernmost) locations characterized by prevalent clear sky (winter snow) conditions showed the worse agreement with a correlation coefficient $r = 0.63$ (0.71), while other stations showed a better correlation ($r = 0.83$ and $r = 85$).

Clear sky ground UV index values for Santiago de Chile have been estimated by means of an empirical reconstruction model, based on noon data from a multichannel radiometer. A ground CMF has been computed as the ratio between measured UV index and modeled clear sky UV index. When comparing the ground CMF with satellite daily (LER-based) CMF for 1996–2011, our results confirm that OMI CMF based on grid cell data introduces significant discrepancy with respect to TOMS CMF, consistently with previous studies carried out with data recorded in European locations (den Outer et al., 2012). On the contrary, the use of overpass LER considerably reduces the inconsistency, although the actual ground CMF values are underestimated (i.e. overestimation of the actual cloud cover conditions) of 10–20% in winter. The trend in reconstructed summer UV index data is found to be $+3.3 \pm 0.9\%$ per decade for the period 1979–2011, while the trend in ground data is $+11.9 \pm 2.5\%$ per decade during the period 1997–2011.

The possible use of the Total Cloud Fraction (TCF) product of MERRA as a proxy of cloudiness in UV reconstruction models is also suggested. A slightly positive trends in summer cloudiness from both satellite and reanalysis data show similar values not statistically significant. It stands out for a good correspondence between LER and TCF but highlights also possible calibration problems in EP TOMS data during 2000–2004 winters.

Acknowledgments

The support of CONICYT-ANILLOS (Preis ACT98), FONDECYT (Preis 3110159 and Preis 1120639), and UTFSM (DGIP 251125) is gratefully acknowledged. Moreover, thanks are due to the principal investigators whose satellite data have been used and to the World Radiation Data Center (WRDC) and to Goddard Earth Sciences Data and Information Services Center (GES DISC).

References

Alados-Arboledas, L., Alados, I., Foyo-Moreno, I., Olmo, F.J., Alcantara, A., 2003. The influence of clouds on surface UV erythemal irradiance. Atmos. Res. 66, 273–290.

Antón, M., Cachorro, V.E., Vilaplana, J.M., Toledano, C., Krotkov, N.A., Arola, A., Serrano, A., de la Morena, B., 2010a. Comparison of UV irradiances from Aura/Ozone Monitoring Instrument (OMI) with Brewer measurements at El Arenosillo (Spain) — part 1: analysis of parameter influence. Atmos. Chem. Phys. 10, 5979–5989.

Antón, M., Vilaplana, J.M., Kroon, M., Serrano, A., Parias, M., Cancillo, M.L., de la Morena, B., 2010b. The empirically corrected EP-TOMS total ozone data against Brewer measurements at El Arenosillo (Southwestern Spain). IEEE Trans. Geosci. Remote Sens. 48 (7), 3039–3045.

Antón, M., Serrano, M., Cancillo, M.L., Garcia, J.A., Madronich, S., 2011a. Empirical evaluation of a simple analytical formula for the ultraviolet index. Photochem. Photobiol. 87, 478–482.

Antón, M., Serrano, M., Cancillo, M.L., Garcia, J.A., Madronich, S., 2011b. Application of an analytical formula for UV Index reconstructions for two locations in Southwestern Spain. Tellus 63B, 1052–1058.

Antón, M., Serrano, A., Cancillo, M.L., Vilaplana, J.M., 2011c. Quality assurance of broadband erythemal radiometers at the Extremadura UV Monitoring Network (Southwestern Spain). Atmos. Res. 100, 83–92.

Balis, D., Kroon, M., Koukouli, M.E., Brinksma, E.J., Labow, G., Veefkind, J.P., et al., 2007. Validation of Ozone Monitoring Instrument total ozone column measurements using Brewer and Dobson spectrophotometer ground-based observations. J. Geophys. Res. 112, D24. http://dx.doi.org/10.1029/2007JD008796.

Bernhard, G., 2011. Trends of solar ultraviolet irradiance at Barrow, Alaska, and the effect of measurement uncertainties on trend detection. Atmos. Chem. Phys. 11, 13029–13045. http://dx.doi.org/10.5194/acp-11-13029-2011.

Bosilovich, M.G., Chen, J., Robertson, F.R., Adler, R.F., 2008. Evaluation of global precipitation in reanalyses. J. Appl. Meteorol. Climatol. 47, 2279–2299.

Bromwich, D.H., Fogt, R.L., Hodges, K.I., Walsh, J.E., 2007. A tropospheric assessment of the ERA-40, NCEP, and JRA-25 global reanalyses in the polar regions. J. Geophys. Res. 112, D10111. http://dx.doi.org/10.1029/2006JD007859.

Buchard, V., Brogniez, C., Auriol, F., Bonnel, B., Lenoble, J., Tanskanen, A., Bojkov, B., Veefkind, P., 2008. Comparison of OMI ozone and UV irradiance data with ground-based measurements at two French sites. Atmos. Chem. Phys. 8, 4517–4528.

Cabrera, S., Ipiña, A., Damiani, A., Cordero, R.R., Piacentini, R., 2012. UV index values and trends in Santiago, Chile (33.5° S) based on ground and satellite data. J. Photochem. Photobiol. B Biol. 115, 73–84.

Chernokulsky, A., Mokhov, I.I., 2012. Climatology of total cloudiness in the Arctic: an intercomparison of observations and reanalyses. Adv. Meteorol. 2012, 542093. http://dx.doi.org/10.1155/2012/542093.

Cordero, R.R., Damiani, A., Dasilva, L., Jorquera, J., Quiroga, M.J., Hernandez, P., Tobar, M., Labbe, F., 2013a. Spectral UV radiance measured at a coastal site. Photochem. Photobiol. Sci. 12, 1193–1201. http://dx.doi.org/10.1039/C3PP25440B.

Cordero, R.R., Damiani, A., Seckmeyer, G., Riechelmann, S., Garate, F., Sanchez, C., Martinez, F., Quiroz, F., Labbe, F., 2013b. Satellite-derived UV climatology at Escudero Station, Antarctic Peninsula. Antarct. Sci. http://dx.doi.org/10.1017/S0954102013000175.

Damiani, A., De Simone, S., Rafanelli, C., Cordero, R.R., Laurenza, M., 2012. Three years of ground-based total ozone measurements in Arctic: comparison with OMI, GOME and SCIAMACHY satellite data. Remote Sens. Environ. 127, 162–180. http://dx.doi.org/10.1016/j.rse.2012.08.023.

Damiani, A., Cabrera, S., Muñoz, R., Cordero, R.R., Labbe, F., 2013. Satellite-derived UV irradiance for a region with complex morphology and meteorology: comparison against ground measurements in Santiago de Chile. Int. J. Remote Sens. 34, 5812–5833. http://dx.doi.org/10.1080/01431161.2013.796101.

den Outer, P.N., Slaper, H., Tax, R.B., 2005. UV radiation in the Netherlands: assessing long-term variability and trends in relation to ozone and clouds. J. Geophys. Res. 110, D02203. http://dx.doi.org/10.1029/2004JD004824.

den Outer, P.N., van Dijk, A., Slaper, H., Lindfors, A.V., De Backer, H., Bais, A.F., Feister, U., Koskela, T., Josefsson, W., 2012. Applying spaceborne reflectivity measurements for calculation of the solar ultraviolet radiation at ground level. Atmos. Meas. Tech. 5, 3041–3054. http://dx.doi.org/10.5194/amt-5-3041-2012.

Eck, T.F., Bhartia, P.K., Kerr, J.B., 1995. Satellite estimation of spectral UVB irradiance using TOMS derived total ozone and UV reflectivity. Geophys. Res. Lett. 22, 611–614. http://dx.doi.org/10.1029/95GL00111.

Hader, D.-P., Kumar, H.D., Smith, R.C., Worrest, R.C., 2007. Effects of solar UV radiation on aquatic ecosystems and interactions with climate change. Photochem. Photobiol. Sci. 6, 267–285. http://dx.doi.org/10.1039/B700020K.

Herman, J.R., Krotkov, N., Celarier, E., Larko, D., Labow, G., 1999. Distribution of UV radiation at the Earth's surface from TOMS-measured UV-backscattered radiances. J. Geophys. Res. 104 (D10), 12,059–12,076.

Herman, J.R., Labow, G., Hsu, N.C., Larko, D., 2009. Changes in cloud and aerosol cover (1980–2006) from reflectivity time series using SeaWiFS, N7-TOMS, EP-TOMS, SBUV-2, and OMI radiance data. J. Geophys. Res. 114, D01201. http://dx.doi.org/10.1029/2007JD009508.

Herman, J.R., DeLand, M.T., Huang, L.-K., Labow, G., Larko, D., Lloyd, S.A., Mao, J., Qin, W., Weaver, C., 2012. A net decrease in the Earth's cloud plus aerosol reflectivity during the past 33 yr (1979–2011) and increased solar heating at the surface. Atmos. Chem. Phys. Discuss. 12, 31991–32038. http://dx.doi.org/10.5194/acpd-12-31991-2012.

Hicke, J.A., Slusser, J., Lantz, K., Pascual, F.G., 2008. Trends and interannual variability in surface UVB radiation over 8 to 11 years observed across the United States. J. Geophys. Res. 113, D21302. http://dx.doi.org/10.1029/2008JD009826.

Ialongo, I., Casale, G.R., Siani, A.M., 2008. Comparison of total ozone and erythemal UV data from OMI with ground-based measurements at Rome

station. Atmos. Chem. Phys. 8, 3283–3289. http://dx.doi.org/10.5194/acp-8-3283-2008.
Ialongo, I., Arola, A., Kujanpää, J., Tamminen, J., 2011. Use of satellite erythemal UV products in analysing the global UV changes. Atmos. Chem. Phys. 11, 9649–9658. http://dx.doi.org/10.5194/acp-11-9649-2011.
Kambezidis, H.D., Adamopoulos, A.D., Zevgolis, D., 2000. Case studies of spectral atmospheric transmittance in the ultraviolet and visible regions in Athens, Greece II. Aerosol transmittance. Atmos. Res. 54, 233–243.
Kazadzis, S., Bais, A., Balis, D., Kouremeti, N., Zempila, M., Arola, A., Giannakaki, E., Amiridis, V., Kazantzidis, A., 2009a. Spatial and temporal UV irradiance and aerosol variability within the area of an OMI satellite pixel. Atmos. Chem. Phys. 9, 4593–4601.
Kazadzis, S., Bais, A., Arola, A., Krotkov, N., Kouremeti, N., Meleti, C., 2009b. Ozone monitoring instrument spectral UV irradiance products: comparison with ground based measurements at an urban environment. Atmos. Chem. Phys. 9, 585–594.
Kleipool, Q.L., Dobber, M.R., de Haan, J.F., Levelt, P.F., 2008. Earth surface reflectance climatology from 3 years of OMI data. J. Geophys. Res. 113, D18308. http://dx.doi.org/10.1029/2008JD010290.
Kondratyev, K.Y., Varotsos, C.A., 1996. Global total ozone dynamics — impact on surface solar ultraviolet radiation variability and ecosystems. Environ. Sci. Pollut. Res. 3, 205–209.
Krotkov, N.A., Herman, J.R., Bhartia, P.K., Fioletov, V., Ahmad, Z., 2001. Satellite estimation of spectral surface UV irradiance 2. Effects of homogeneous clouds and snow J. Geophys. Res. 106, 11743–11759.
Kylling, A., Albold, A., Seckmeyer, G., 1997. Transmittance of a cloud is wavelength-dependent in the UV-range: Physical interpretation. Geophys. Res. Lett. 24 (4), 397–400.
Labow, G.J., Herman, J.R., Huang, L.-K., Lloyd, S.A., DeLand, M.T., Qin, W., Mao, J., Larko, D.E., 2011. Diurnal variation of 340 nm Lambertian equivalent reflectivity due to clouds and aerosols over land and oceans. J. Geophys. Res. 116, D11202. http://dx.doi.org/10.1029/2010JD014980.
Lefèvre, M., Oumbe, A., Blanc, P., Espinar, B., Gschwind, B., Qu, Z., Wald, L., Schroedter-Homscheidt, M., Hoyer-Klick, C., Arola, A., Benedetti, A., Kaiser, J.W., Morcrette, J.-J., 2013. McClear: a new model estimating downwelling solar radiation at ground level in clear-sky conditions. Atmos. Meas. Tech. Discuss. 6, 3367–3405. http://dx.doi.org/10.5194/amtd-6-3367-2013.
Lindfors, A., Kaurola, J., Arola, A., Koskela, T., Lakkala, K., Josefsson, W., Olseth, J.A., Johnsen, B., 2007. A method for reconstruction of past UV radiation based on radiative transfer modeling: applied to four stations in northern Europe. J. Geophys. Res. 112, D23201. http://dx.doi.org/10.1029/2007JD008454.
Madronich, S., 2007. Analytic formula for the clear-sky UV index. Photochem. Photobiol. 83, 1537–1538. http://dx.doi.org/10.1111/j.1751-1097.2007.00200.x.
Matthijsen, J., Slaper, H., Reinen, H.A.J.M., Velders, G.J.M., 2000. Reduction of solar UV by clouds: a comparison between satellite-derived cloud effects and ground-based radiation measurements. J. Geophys. Res. 105 (D4), 5069–5080.
McKinlay, A.F., Diffey, B.L., 1987. A reference action spectrum for ultraviolet induced erythema in human skin, in: Commission International de l'Éclairage (CIE). Res. Note 6, 17–22.
Montecinos, A., Aceituno, P., 2003. Seasonality of the ENSO-related rainfall variability in central Chile and associated circulation anomalies. J. Clim. 16, 281–296.
Ogunjobi, K.O., Kim, Y.J., 2004. Ultraviolet (0.280–0.400 μm) and broadband solar hourly radiation at Kwangju, South Korea: analysis of their correlation with aerosol optical depth and clearness index. Atmos. Res. 71, 193–214.
Slaper, H., Velders, G.J.M., Daniel, J.S., de Gruijl, F.R., van der Leun, J.C., 1996. Estimates of ozone depletion and skin cancer incidence to examine the Vienna Convention achievements. Nature 384, 256–258. http://dx.doi.org/10.1038/384256a0.
Staiger, H., Kaurola, J., de Backer, H., 2010. Gridded daily European solar cloud modification factors derived from ERA-40 information and pyranometer observations. J. Geophys. Res. 115, D21109. http://dx.doi.org/10.1029/2009JD013718.
Tanskanen, A., Lindfors, A., Määttä, A., Krotkov, N., Herman, J., Kaurola, J., Koskela, T., Lakkala, K., Fioletov, V., Bernhard, G., McKenzie, R., Kondo, Y., M., O'Neill, Slaper, H., den Outer, P., Bais, A.F., Tamminen, J., 2007. Validation of daily erythemal doses from Ozone Monitoring Instrument with ground-based UV measurement data. J. Geophys. Res. 112, D24S44. http://dx.doi.org/10.1029/2007JD008830.
Tevini, M., 1993. UV-B Radiation and Ozone Depletion: Effect on Humans, Animals, Plants, Microorganisms and Materials. Lewis, New York.
Weihs, P., Blumthaler, M., Rieder, H.E., Kreuter, A., Simic, S., Laube, W., Schmalwieser, A.W., Wagner, J.E., Tanskanen, A., 2008. Measurements of UV irradiance within the area of one satellite pixel. Atmos. Chem. Phys. 8, 5615–5626.
World Meteorological Organization (WMO), 2007. Scientific assessment of ozone depletion: 2006. Global Ozone Res. and Monit. Proj. WMO Rep., 50 (Geneva).
Yang, K., Krotkov, N.A., Bhartia, P.K., Joiner, J., McPeters, R., Krueger, A.J., Vasilkov, A., Taylor, S., Haffner, D., Chiou, E., 2008. Satellite ozone retrieval with improved radiative cloud pressure. Proc. Quadrennial Ozone Symp., Tromso, Norway.
Zib, B.J., Dong, X., Xi, B., Kennedy, A., 2012. Evaluation and intercomparison of cloud fraction and radiative fluxes in recent reanalyses over the arctic using BSRN surface observations. J. Clim. 25, 2291–2305.
Ziemke, J.R., Chandra, S., Herman, J., Varotsos, C., 2000. Erythemally weighted UV trends over northern latitudes derived from Nimbus 7 TOMS measurements. J. Geophys. Res. 105, 7373–7382.